Available online at www.sciencedirect.com
SCIENCE DIRECT®
Journal of Solid State Chemistry 176 (2003) 213–220
JOURNAL OF SOLID STATE CHEMISTRY
http://elsevier.com/locate/jssc

# Structural order and disorder in Co-based layered cuprates $CoSr_2(Y,Ce)_sCu_2O_{5+2s}$ ($s = 1-3$)

T. Nagai,[a,*] V.P.S. Awana,[a] E. Takayama-Muromachi,[a] A. Yamazaki,[b] M. Karppinen,[c] H. Yamauchi,[c] S.K. Malik,[d] W.B. Yelon,[e] and Y. Matsui[a,b]

[a] *National Institute for Materials Science, 1-1 Namiki, Tsukuba, Ibaraki 305-0044, Japan*
[b] *Department of Resources and Environmental Engineering, Waseda University, 3-4-1 Ohkubo, Shinjuku, Tokyo 169-8555, Japan*
[c] *Materials and Structures Laboratory, Tokyo Institute of Technology, Yokohama 226-8503, Japan*
[d] *Tata Institute of Fundamental Research, Homi Bhabha Road, Mumbai 400005, India*
[e] *Graduate Center for Materials Research, University of Missouri-Rolla, MO 65409, USA*

Received 25 February 2003; received in revised form 11 July 2003; accepted 24 July 2003

**Abstract**

Crystal structures of a homologous series of Co-based layered cuprates, $CoSr_2(Y,Ce)_sCu_2O_{5+2s}$ ($s = 1-3$), have been investigated by high-resolution electron microscopy (HREM) and electron diffraction (ED) techniques. For all the three phases ED patterns showed double periodicity along a direction parallel to the CoO layers, indicating a regular alternation of two types of $CoO_4$-tetrahedra chains within the layers. Also seen was ordering of the chains along the layer-stacking direction for the $s = 1$ phase (Co-1212); ED patterns simulated based on the proposed superstructure model well reproduced the observed patterns. For the $s = 2$ (Co-1222) and $s = 3$ (Co-1232) phases in which an additional fluorite-type layer-block is inserted between two $CuO_2$ planes, HREM and ED analysis revealed complete disorder of the $CoO_4$ chains along the layer-stacking direction. This implies that the interlayer ordering is mainly controlled by the distance between the neighboring CoO layers.


*Keywords:* Co-based cuprates; Fluorite-type block; Superstructure; Electron diffraction; High-resolution electron microscopy

## 1. Introduction

The well-known high-$T_c$ superconductor, $YBa_2Cu_3O_7$ (Cu-1212 or so-called "123") accepts various elemental substitutions. Such substitutions have resulted in discoveries of a large number of related phases. Among the *M*-1212 phases, where the CuO layer of the Cu-1212 phase is replaced by an *M*O layer, those with *M*= Ga, Al, or Co have attracted significant interest as in their crystal structures oxygen atoms tetrahedrally coordinate the *M* atoms to form chains of corner-sharing $MO_4$ tetrahedra [1–6]. Several authors have reported the presence of complicated superstructures due to ordering of two types of $MO_4$-tetrahedra chains, *L*- and *R*-chains, where the tetrahedra rotate in different ways [4–6]. In this paper, we present results of electron diffraction (ED) and high-resolution electron microscopy (HREM) investigation for a whole homologous series of *M*= Co compounds, i.e. Co-12*s*2 phases ($s = 1-3$) with compositions of $CoSr_2YCu_2O_{7-\delta}$, $CoSr_2(Y_{3/4}Ce_{1/4})_2Cu_2O_{9-\delta}$, and $CoSr_2(Y_{1/3}Ce_{2/3})_3Cu_2O_{11-\delta}$. The Co-1222 phase has a three-layer fluorite-type $(Y_{3/4}Ce_{1/4})$–$O_2$–$(Y_{3/4}Ce_{1/4})$ block to replace the single, oxygen-free Y (or rare earth, RE) layer of the Co-1212 phase, whereas the Co-1232 phase accommodates a five-layer $(Y_{1/3}Ce_{2/3})$–$O_2$–$(Y_{1/3}Ce_{2/3})$–$O_2$–$(Y_{1/3}Ce_{2/3})$ block between the two $CuO_2$ planes. With increasing number of *s* (from 1 to 3), the distance between the CoO layers increases since the thickness of the RE-containing block increases. We have revealed both structural order and disorder of the two different types of $CoO_4$ chains in the Co-12*s*2 phases. The findings are discussed with respect to the distance between the neighboring CoO layers.

## 2. Experimental

The $CoSr_2(Y,Ce)_sCu_2O_{5+2s-\delta}$ (Co-12*s*2) compounds were synthesized through a solid-state reaction route

*Corresponding author. Fax: +81-29-851-4976.
*E-mail address:* nagai.takuro@nims.go.jp (T. Nagai).

0022-4596/$ - see front matter © 2003 Elsevier Inc. All rights reserved.
doi:10.1016/S0022-4596(03)00412-2

from $Co_2O_3$, $SrO_2$, $Y_2O_3$, $CeO_2$ and CuO. Calcinations were carried out on mixed powders at 975°C and 1000°C, each for 24 h with an intermediate grinding. The pressed bar-shape pellets were annealed in flowing oxygen at 1010°C for 40 h and subsequently cooled slowly over a span of another 20 h to room temperature. For the Co-1222 and Co-1232 compounds, additional heat treatments at temperatures 10–20°C higher than those for the Co-1212 compound were necessary at each heating step to obtain the desired phase. Previously the same samples were characterized by wet-chemical and thermogravimetric analyses, and found stoichiometric in terms of their oxygen contents [7].

For the Co-1212 and Co-1232 compounds, all X-ray diffraction maxima could be indexed on the basis of $I2cm$ (No. 46) orthorhombic symmetry [1,3] and lattice parameters, $a = 0.5409$ nm, $b = 0.5452$ nm, $c = 2.2799$ nm (Co-1212), and $a = 0.5417$ nm, $b = 0.5469$ nm, $c = 3.3231$ nm (Co-1232). For the Co-1222 compound, the lattice parameters $a_{p2} = b_{p2} = 0.3832$ nm and $c_{p2} = 2.8170$ nm were given with use of $I4/mmm$ (No. 139) tetragonal symmetry of primitive 1222 structure. The ED patterns and HREM images were obtained using a super-high-voltage transmission electron microscope (Hitachi H-1500) operated at an accelerating voltage of 820 kV. The TEM specimens were prepared by crashing the synthesized samples into fine fragments, which were ultrasonically dispersed in $CCl_4$ and transferred to carbon microgrids. Simulations of ED patterns and HREM images based on dynamical diffraction theory were carried out with MacTempas software.

## 3. Results and discussion

Fig. 1a shows an ED pattern taken along [001] direction for the Co-1212 phase. The main spots are produced by the basic perovskite structure, and can be indexed on a rectangular quasi-square mesh, diagonal relative to the basic perovskite mesh ($a \approx b = \sqrt{2}a_p$) [4]. Additionally, superstructural spots are seen along the $b^*$-axis indicating double periodicity of $b_s = 2b$. The spots can be indexed as $(h, k \pm \frac{1}{2}, 0)$. In Fig. 1b shown is the ED pattern for the same sample along [100] direction, where the $(0, k \pm \frac{1}{2}, 0)$ superstructural spots that are clearly visible in Fig. 1a are absent. The $(0, k \pm \frac{1}{2}, 0)$ superlattice reflections in Fig. 1a are kinematically forbidden but induced by multiple scattering of electron beam. The strong $0\,k\,l$ fundamental reflections with $k$, $l$= even in Fig. 1b are caused by the primitive 1212 structure with a $c$-axis parameter of $c_{p1} \approx 3a_p$. We can see other relatively weak $0\,k\,l$ reflections with $k$, $l$= odd too, which indicate that the $c$-axis parameter of the Co-1212 phase is twice in length as compared with that of the primitive 1212 structure unit, $c = 2c_{p1} \approx 6a_p$. Ignoring the superlattice reflections indicating $b_s = 2b$, the reciprocal lattice is face-centered and hence the real lattice is body-centered, which leads to a shift of the $CoO_4$ chain position by $[\frac{1}{2}\frac{1}{2}0]$ from the neighboring CoO layer. The superlattice reflections in Fig. 1a showing double periodicity along the $b$ direction are indicative of a regular alternation of two different types of symmetry ($L$ and $R$) of the $CoO_4$-tetrahedra chains along the direction as shown in Fig. 2a [4]. It has been reported that $MO_4$-tetrahedra can rotate in two different ways about the $c$-axis, giving rise to the formation of two kinds of zig-zag chains, $L$-chains and $R$-chains [4]. The $L - R$ distinction is just relative because an $L$-chain is transferred into an $R$-chain by a mirror operation, and hence the two types of chains are energetically equivalent, and would thus form with equal probabilities.

In order to reveal the arrangement of the chains along the layer-stacking direction ($c$ direction), superlattice reflections were observed along a direction perpendicular to the direction. The obtained ED pattern is shown in Fig. 2b. The superspots, $(1, \frac{1}{2}, l)$ and $(3, \frac{3}{2}, l)$, are only slightly streaked along the $c^*$ direction, which indicates that the two types of chains are nearly ordered along the $c$ direction. The interval between the neighboring superspots shows that the periodicity of the ordering is equal to the $c$-axis parameter, $c_s = c$.

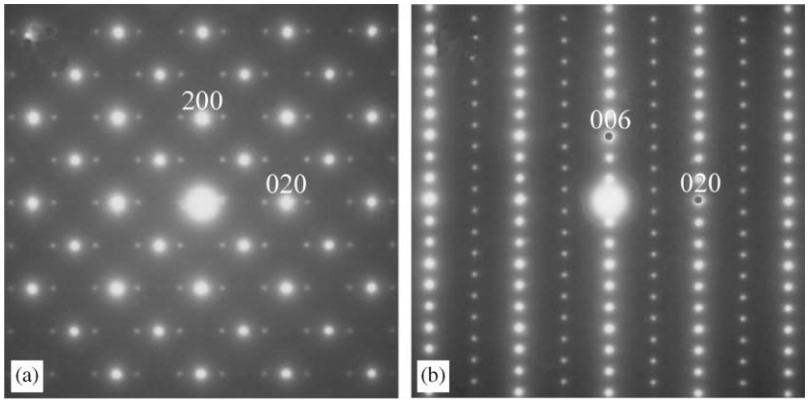


Fig. 1. ED patterns taken along (a) [001] and (b) [100] direction for the Co-1212 phase, $CoSr_2YCu_2O_7$. The main spots are indexed in the subcell.

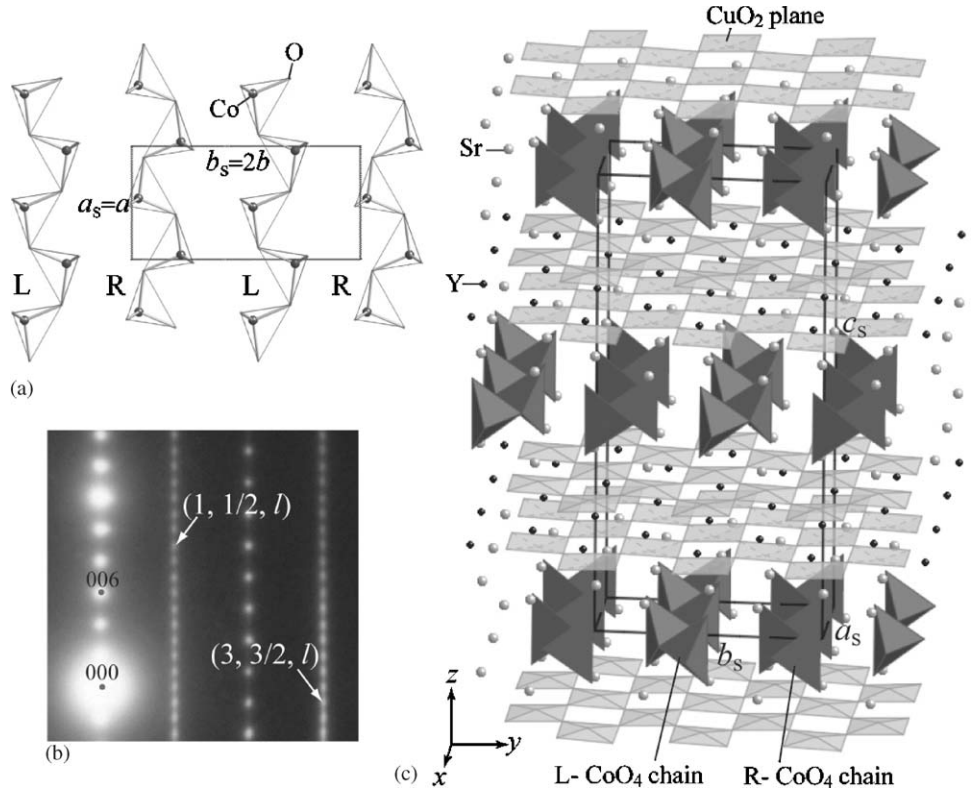


Fig. 2. (a) Illustration of a regular alternation of two types of $CoO_4$-tetrahedra chains, *L*-and *R*-chains, along the *b* direction. (b) ED pattern taken along $[1\bar{2}0]$ for the Co-1212 phase. (c) Superstructure model proposed for the Co-1212 phase with *P*2*cm* (No. 28) orthorhombic symmetry and lattice parameters, $a_s = a$, $b_s = 2b$, and $c_s = c$. The positional parameters were adapted from those proposed for Ga-1212 by Roth et al. [1], which are given for *Ima*2 (No. 46) orthorhombic unit cell with $b \approx c = \sqrt{2}a_p$.

We display in Fig. 2c the proposed superstructure model with *P*2*cm* (No. 28) orthorhombic symmetry and lattice parameters, $a_s = a$, $b_s = 2b$, and $c_s = c$. The positional parameters were adapted from those proposed for $GaSr_2YCu_2O_7$ (Ga-1212) by Roth et al. [1], which are based on *Ima*2 (No. 46) orthorhombic symmetry with cell setting of $b \approx c = \sqrt{2}a_p$. The superstructure model gave simulated ED patterns consistent with the experimentally observed ones, as shown in Fig. 3. Especially, Figs. 3b and c well produce the aforementioned striking feature that the (0, $k \pm \frac{1}{2}$, 0) superlattice reflections are induced in [001] projection whereas they are not induced in [100] projection. (It can be deduced that the local crystal areas have slight deviations from exact [001] zone-axis orientation when the pattern shown in Fig. 1a is observed.) Fig. 4 shows HREM images taken along (a) $[1\bar{1}0]$ and (b) [100] directions (in the subcell setting) for the Co-1212 phase. The $[1\bar{1}0]$ zone-axis ED pattern is inset in Fig. 4a and a simulated HREM image based on the superstructure model is inset in each figure. The 1212-type stacking of layers along the *c*-axis, (SrO–CoO–SrO–$CuO_2$–Y–$CuO_2$), is clearly observed in Fig. 4a. Fig 4b shows the $[\frac{1}{2}\frac{1}{2}0]$ relative shift of the $CoO_4$ chain position between neighboring CoO layers. In this figure, the white dot indicated by an arrow corresponds to a chain of oxygen vacancies between neighboring $CoO_4$ chains in a CoO layer.

The phenomenon discussed for the Co-1212 phase, i.e. ordering of $CoO_4$ chains, is observed also for the Co-1222 phase. The [001] and [100] zone-axis ED patterns are shown in Figs. 5a and b, where the main spots are indexed on a diagonal mesh parallel to the case of Fig. 1. In Fig. 5a, the reflections come from two different areas of the crystal, namely, orientation variants differing by a 90° rotation about the *c*-axis. The striking difference between Figs. 1a and 5a is that the $h\,k\,0$ fundamental reflections with $h$, $k$ = odd are present in Fig. 1a but absent in Fig. 5a. This is due to the presence of the three-layer fluorite-type block, causing a relative shift over $[\frac{1}{2}00]$ or $[0\frac{1}{2}0]$ of the two neighboring blocks. There are relatively weak $h\,k\,0$ fundamental reflections with $h$= odd, $k$= even and the corresponding ones appear in the 90°-rotated positions, because of the twin domain structure. Also the weak superlattice reflections indicating the double periodicity of $b_s = 2b$ due to the regular alternation of *L*-and *R*-type chains can be seen, and the corresponding ones appear in the rotated positions as well. In Fig. 5b only seen are the $0\,k\,l$ reflections with $k + l$= even, which indicates that the *c*-axis parameter of the Co-1222 phase is equal to that of the primitive 1222 structure unit, $c = c_{p2} \approx 6a_p + 2c_f$ ($c_f$: thickness of

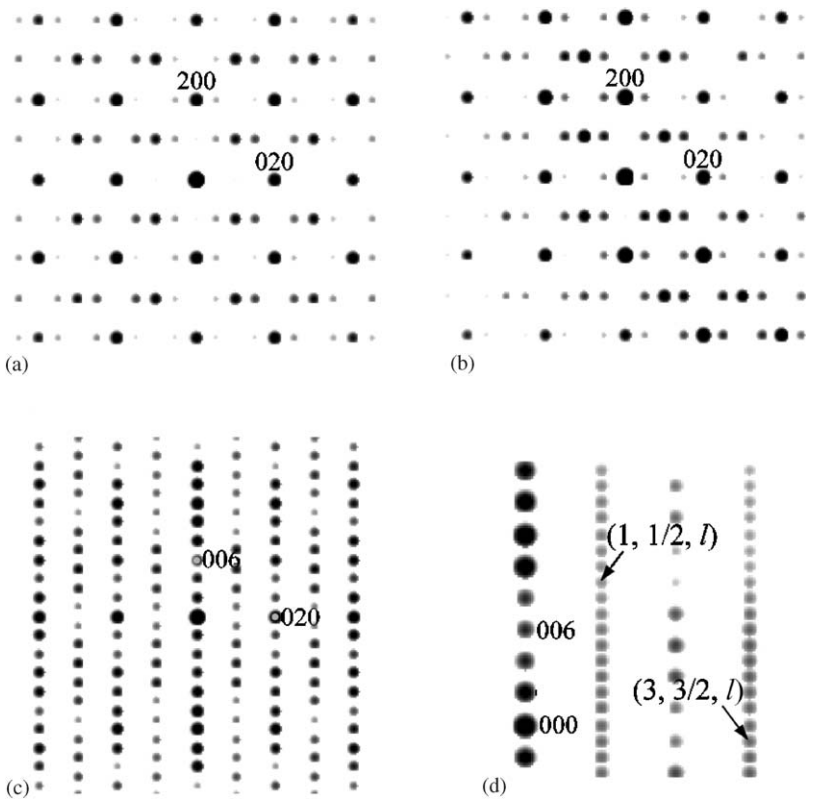


Fig. 3. Simulated ED patterns using the superstructure model shown in Fig. 2c. The main spots are indexed in the subcell. (a) [001] projection (in the subcell setting) with no crystal tilt, $h = k = 0$ mrad, (b) [001] projection with slight crystal tilt, $h = k = 20$ mrad, (c) [100] projection, (d) $[1\bar{2}0]$ projection ((c), (d): with no crystal tilt). All the simulations were carried out with crystal thickness, $t = 10$ nm.

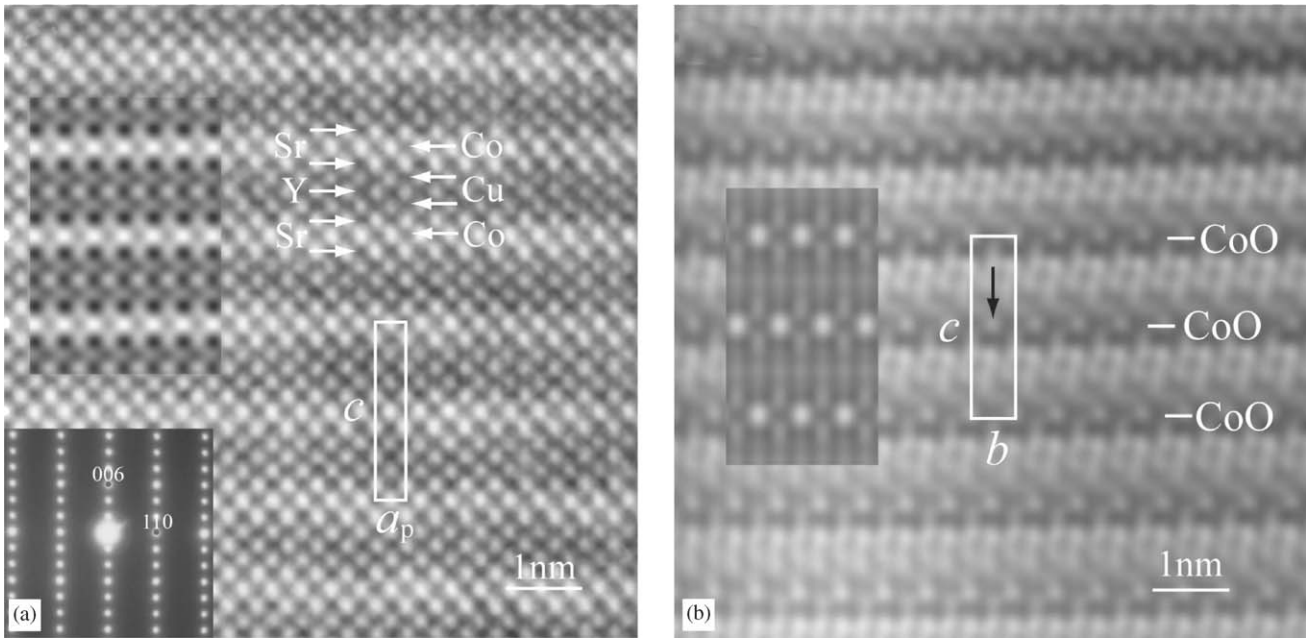


Fig. 4. HREM images for the Co-1212 phase projected along (a) $[1\bar{1}0]$ and (b) [100] (in the subcell setting). The $[1\bar{1}0]$ zone-axis ED pattern is inset in figure (a) and a simulated HREM image is inset in each figure. The simulations were carried out with crystal thickness, $t = 2$ nm, and defocus, $\Delta f = -44$ nm. In figure (b), the white dot indicated by an arrow corresponds to a chain of oxygen vacancies between neighboring $CoO_4$ chains in a CoO layer.

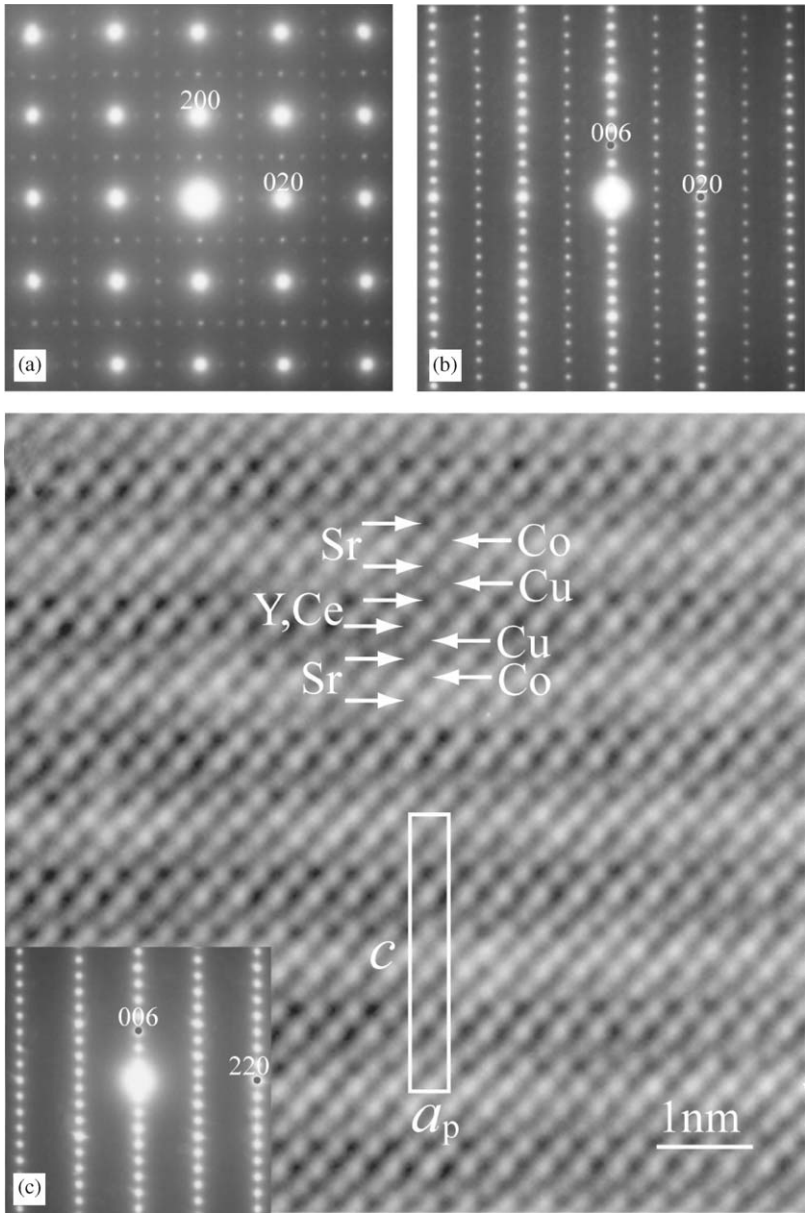


Fig. 5. ED patterns taken along (a) [001] and (b) [100] direction and (c) HREM image projected along $[1\bar{1}0]$ for the Co-1222 phase, $CoSr_2(Y_{3/4}Ce_{1/4})_2Cu_2O_9$.

fluorite-type RE-$O_2$-RE block), and the unit cell includes two CoO layers. The extinction condition for fundamental reflections due to the lattice type, $k+l=$ odd, makes the basic lattice A-face-centered, which is indicative of a position shift of the $CoO_4$ chain by $[0\frac{1}{2}0]$ between the neighboring CoO layers. Fig. 5c shows the HREM image taken along $[1\bar{1}0]$ direction. The 1222-type stacking of layers is clearly seen, with a relative shift of the blocks due to the fluorite-type $(Y_{3/4}Ce_{1/4})$–$O_2$–$(Y_{3/4}Ce_{1/4})$ block.

For the Co-1232 phase, the ED patterns along [001] and [100], and the HREM image along $[1\bar{1}0]$ are shown in Figs. 6a–c, respectively. In Fig. 6a, the reflections come from twin domains like in the case of the Co-1222 phase, and the pattern from the single-crystal domain is identical to the one in Fig. 1a, showing $b_s = 2b$. The five-layer fluorite-type block gives rise to no relative shift of the two neighboring blocks [8], which explains the prominent presence of the $h\,k\,0$ reflections with $h$, $k=$ odd. The $0\,k\,l$ reflections with $k$, $l=$ odd indicate that the $c$-axis parameter of the Co-1232 phase is doubled as compared with that of the primitive 1232 structure unit, $c = 2c_{p3} \approx 6a_p + 4c_f$. Parallel to the case of the Co-1212 phase, this phase has a body-centered lattice of fundamental structure, indicating that the $CoO_4$ chain position shifts by $[\frac{1}{2}\frac{1}{2}0]$ between the neighboring CoO layers. We can see in Fig. 6c the 1232-type stacking of layers, with no relative shift due to the fluorite-type $(Y_{1/3}Ce_{2/3})$–$O_2$–$(Y_{1/3}Ce_{2/3})$–$O_2$–$(Y_{1/3}Ce_{2/3})$ block.

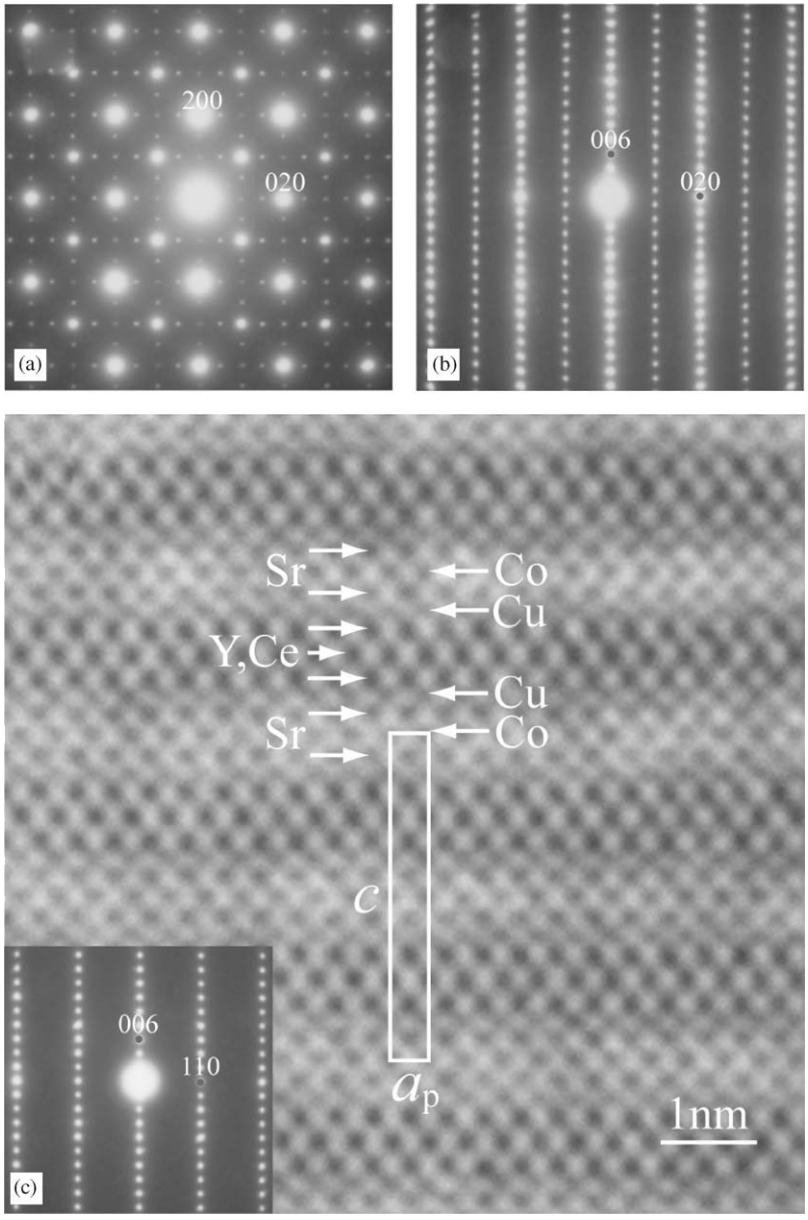


Fig. 6. ED patterns taken along (a) [001] and (b) [100] direction and (c) HREM image projected along $[1\bar{1}0]$ for the Co-1232 phase, $CoSr_2(Y_{1/3}Ce_{2/3})_3Cu_2O_{11}$.

As described above, the intralayer ordering of the two types of chains is a general phenomenon for all the three phases. For the Co-1212 phase, the chains are furthermore ordered along the $c$ direction. Now, let us discuss the chain arrangement along the $c$ direction in case of the Co-1222 and 1232 phases, which have the fluorite-type block between $CuO_2$ planes. The ED patterns observed along a direction perpendicular to the $c$ direction are shown in Fig. 7. For both phases, the superspots, $(1, \frac{1}{2}, l)$ and $(3, \frac{3}{2}, l)$, are completely streaked, that is, there exists no periodic variation along the $c^*$ direction in intensity of the streaks. This feature indicates that the chains are completely disordered along the $c$ direction. We display in Fig. 8 an HREM image for the Co-1232 projected along $[1\bar{2}0]$, corresponding to the ED pattern in Fig. 7b. The observed dot rows perpendicular to the $c$ direction were formed by the completely streaked superlattice reflections, as judged by the regular interval of $2d_{210}$ between the neighboring dots. The arrangement of dots shows the intralayer ordering and interlayer disordering of the $CoO_4$ chains in the phase.

Ordering of the two types of chains presumably occurs so that the total lattice energy would be reduced. Schematic representations of $CoO_4$ chain arrangement for the present Co-12$s$2 phases are shown in Fig. 9. For all the three phases, the intralayer interaction between the chains is strong because of shortness of the distance

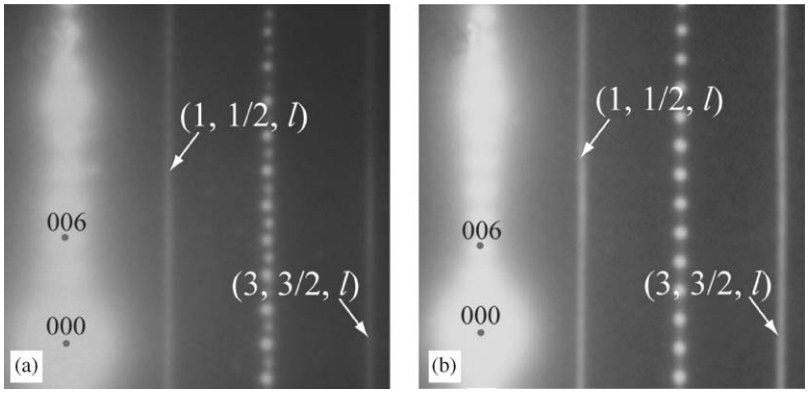


Fig. 7. ED patterns taken along [1$\bar{2}$0] for (a) the Co-1222 phase and (b) the Co-1232 phase.

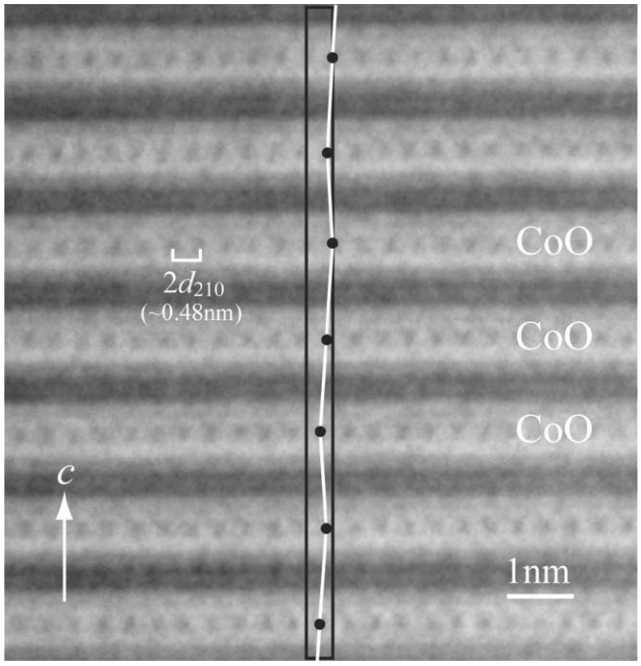


Fig. 8. HREM image for the Co-1232 phase projected along [1$\bar{2}$0], corresponding to the ED pattern in Fig. 7b. The arrangement of dots shows the intralayer ordering and interlayer disordering of the $CoO_4$ chains.

between them. This is the reason for the general phenomenon of intralayer ordering of the two types of chains. On the other hand, the distance across the SrO–$CuO_2$–(Y,Ce)–($O_2$–(Y,Ce))$_{s-1}$–$CuO_2$–SrO block is long and the interlayer interaction thus weak. For the $s = 2$ and 3 phases, the distance is 1.41 nm (Co-1222) or 1.66 nm (Co-1232), and the interaction is especially weak, which probably causes the complete lack of interlayer order of the $CoO_4$ chains.

None of the three samples showed superconductivity. The magnetization data obtained for the samples are given and discussed elsewhere [7,9]. The data showed a general behavior common to all the three phases that is believed to originate from short-range low-dimensional correlations among the Co spins within the CoO layer.

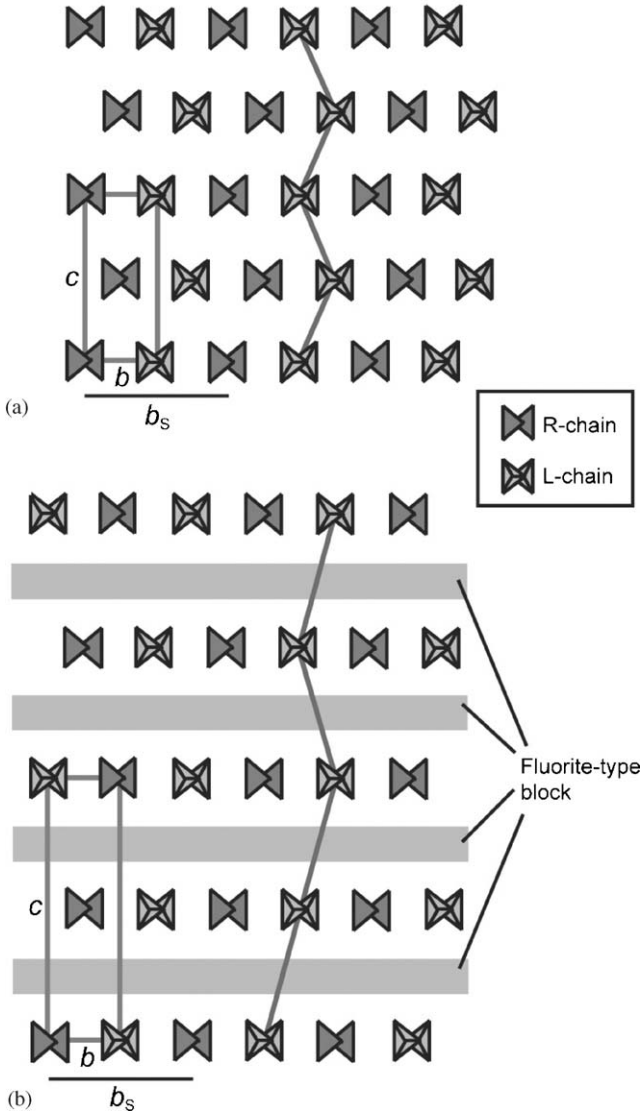


Fig. 9. Schematic representations of the arrangement of *R*- and *L*-$CoO_4$ chains for (a) the Co-1212 phase and (b) the Co-1222 and Co-1232 phases.

Such short-range low-dimensional correlations are not likely to be affected by the differences in the interlayer interactions of the $CoO_4$ chains, the fact of which explains the observed common behavior. The lack of superconductivity in the samples is primarily attributed to the fact that appropriate doping of the $CuO_2$ planes with holes has not yet been achieved for the Co-12$s$2 phases. Here it should be noted that our preliminary Cu $L$-edge X-ray absorption near-edge structure (XANES) spectroscopy study revealed that the valence of Cu is very close to II in all the three samples [10].

## 4. Conclusion

We revealed the structural order and disorder concerning two different types of $CoO_4$ tetrahedra chains, $L$-and $R$-chains, in the homologous series of Co-based cuprates, Co-12$s$2 ($s = 1-3$). Intralayer ordering of the chains was found common to all the three phases. We also revealed a difference in the interlayer arrangement between the $s = 1$ phase (without fluorite-type blocks) and the $s = 2$ and 3 phases (with the blocks): along the layer-stacking direction the chains are nearly ordered for the former phase, but completely disordered for the latter two phases. The finding implies that the expansion of the distance between CoO layers, making the interlayer interaction weak, mainly causes the loss of the interlayer ordering.

## Acknowledgments

We thank K. Kimoto, T. Asaka and C. Tsuruta for helpful discussions. This work was supported by the Nanotechnology Support Project of the MEXT, Japan.

## References

[1] G. Roth, P. Adelmann, G. Heger, R. Knitter, T. Wolf, J. Phys. 1 (1991) 721.
[2] J.T. Vaughey, J.P. Thiel, E.F. Hasty, D.A. Groenke, C.L. Stern, K.L. Poeppelmeier, B. Dabrowski, P. Radaelli, A.W. Mitchel, D.G. Hinks, Chem. Mater. 3 (1991) 935.
[3] Q. Huang, R.J. Cava, A. Santoro, J.J. Krajewski, W.F. Peck, Physica C 193 (1992) 196.
[4] T. Krekels, O. Milat, G. Van Tendeloo, S. Amelinckx, T.G.N. Babu, A.J. Wright, C. Greaves, J. Solid State Chem. 105 (1993) 313.
[5] J. Ramirez-Castellanos, Y. Matsui, E. Takayama-Muromachi, M. Isobe, J. Solid State Chem. 123 (1996) 378.
[6] J. Ramirez-Castellanos, Y. Matsui, M. Isobe, E. Takayama-Muromachi, J. Solid State Chem. 133 (1997) 434.
[7] M. Karppinen, V.P.S. Awana, Y. Morita, H. Yamauchi, Physica C, 2003, in press.
[8] T. Wada, A. Nara, A. Ichinose, H. Yamauchi, S. Tanaka, Physica C 192 (1992) 181.
[9] V.P.S. Awana, S.K. Malik, W.B. Yelon, M. Karppinen, H. Yamauchi, Physica C 378 (2002) 155.
[10] M. Karppinen, Y. Morita, V.P.S. Awana, H. Yamauchi, R.S. Liu, J.M. Chen, unpublished.